

Review

Iridaaromatics via Methoxy(alkenyl)carbeneiridium Complexes

Maria Talavera ^{1,2}  and Sandra Bolaño ^{2,*} 

¹ Department of Chemistry, Humboldt-Universität zu Berlin, Brook-Taylor-Str. 2, 12489 Berlin, Germany; talaverm@hu-berlin.de

² Departamento de Química Inorgánica, Universidade de Vigo, Campus Universitario, 36310 Vigo, Spain

* Correspondence: bgs@uvigo.es

Abstract: This review describes the development of a versatile methodology to synthesize polycyclic metallaaromatic hydrocarbons based on iridium, as well as the studies that helped us to determine and understand what is required in order to broaden the scope and the selectivity of the methodology and stabilize the complexes obtained. This methodology aims to open the door to new materials based on graphene fragments.

Keywords: metallaaromatics; iridium; PAHs



Citation: Talavera, M.; Bolaño, S. Iridaaromatics via Methoxy (alkenyl)carbeneiridium Complexes. *Molecules* **2021**, *26*, 4655. <https://doi.org/10.3390/molecules26154655>

Academic Editors:
Maurizio Peruzzini and
Luca Gonsalvi

Received: 10 July 2021
Accepted: 28 July 2021
Published: 31 July 2021

Publisher's Note: MDPI stays neutral with regard to jurisdictional claims in published maps and institutional affiliations.



Copyright: © 2021 by the authors. Licensee MDPI, Basel, Switzerland. This article is an open access article distributed under the terms and conditions of the Creative Commons Attribution (CC BY) license (<https://creativecommons.org/licenses/by/4.0/>).

1. Introduction

The interest of graphene lies in its structure and unusual physical properties, which turn polycyclic aromatic hydrocarbons (PAHs) and nanographenes, small graphene fragments, into the subject of several research in the last decades [1]. Studying PAHs allows for correlating their geometrical and electronic structure with their properties, which can then be applied to larger structures. It has been found that the introduction of defects or irregularities in the structure of PAHs modifies their properties and consequently broadens their field of application. Among these defects, the most common are deviations from planarity due to edges, the introduction of non-six-member rings, doping with heteroatoms or the inclusion of substituents for their functionalization [2–5].

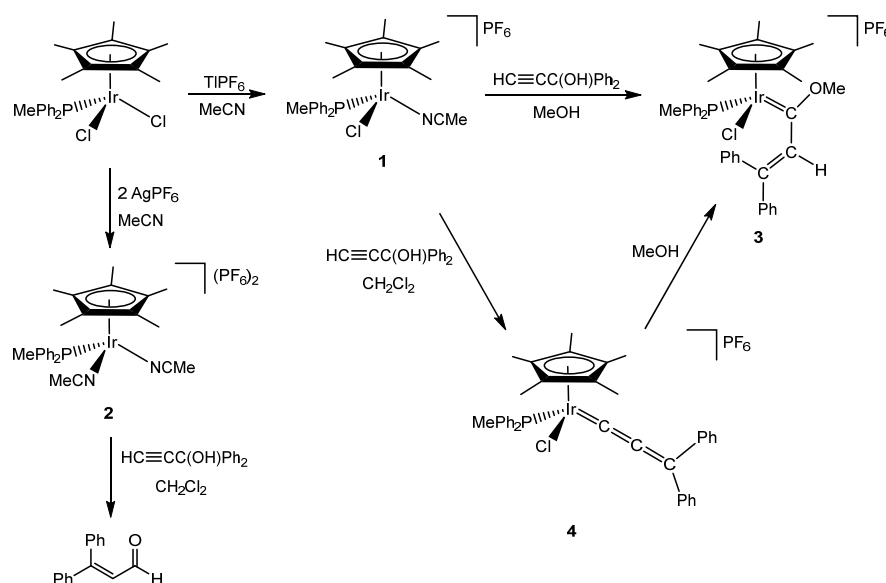
The introduction of these irregularities in PAHs can lead to new materials improving results and even opening up new applications with respect to their non-defective analogues. With this in mind, over the last decade our research group has focused its interest on the development of new PAHs by incorporating a transition metal in order to create polycyclic metallaaromatic hydrocarbons (PMAHs) by replacing a CH unit with a transition metal. These new systems are considered to be doped PAHs and could potentially introduce a slight deviation of the plane. This has led us to develop a synthetic and versatile methodology that allows us to obtain PMAHs with different structures and sizes, as this is the key to obtaining new and improved properties for their application in the field of materials.

In this review, we focus on the studies which led us to the successful development and understanding of a methodology for synthesizing iridium based PMAHs.

2. Methoxy(alkenyl)carbeneiridium Complexes

The synthesis of methoxycarbenes is a well-known process which is achieved by the nucleophilic addition of methanol to a vinylidene or allenylidene complex [6,7]. One useful methodology to obtain these products is the activation of terminal alkynes and propargylic alcohols with a suitable precursor. In this regard, complexes with labile ligands, such as ethylene, cyclooctadiene or acetonitrile, are convenient starting materials [8]. Therefore, the acetonitrile complexes [IrCp*Cl(NCMe)(PPh₂Me)]PF₆ (**1**) and [IrCp*(NCMe)₂(PPh₂Me)](PF₆)₂ (**2**) obtained from [IrCp*Cl₂(PPh₂Me)] (Scheme 1) promised to be suitable precursors. It was observed that the chosen salt for the abstraction of the chlorido ligand played a key role in the product selectivity. Therefore, AgPF₆

promotes a double methathesis (independent of the stoichiometry) while TlPF₆ selectively leads to the monoacetonitrile derivative [9,10].

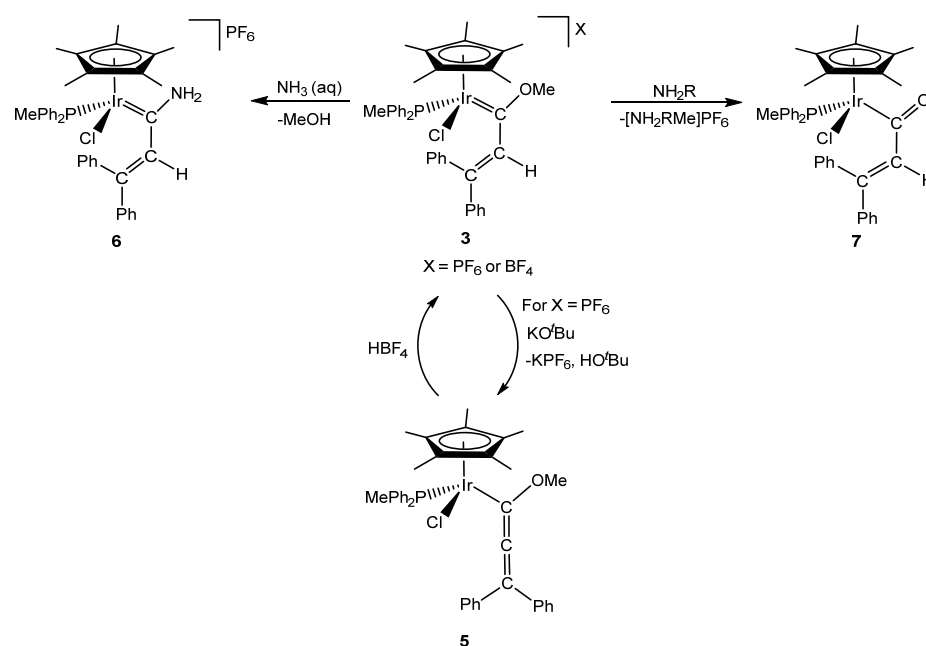


Scheme 1. Synthesis of the acetonitrile complexes 1 and 2 and their reactivity towards propargylic alcohols.

The monoacetonitrile complex 1 reacted with 1,1-diphenyl-2-propyn-1-ol in methanol, yielding the expected methoxy(alkenyl)carbeneiridium complex [IrCp*Cl{=C(OMe)CH=CPh₂}(PPh₂Me)]PF₆ (3). When the reaction was performed in dichloromethane, the formation of an unstable allenylidene complex 4 was observed, which by addition of methanol yielded, as proposed, complex 3 (Scheme 1) [9].

Interestingly, the bisacetonitrile complex 2 was capable of catalytically activating propargylic alcohols in order to produce the corresponding aldehydes through a Meyer–Schuster rearrangement, instead of the expected organometallic derivative (Scheme 1). The mechanism proposed for the reaction involved the initial formation of a vinylidene complex which underwent an intramolecular nucleophilic addition of the hydroxo group to the α -carbon of the vinylidene [10]. This mechanism excluded the formation of an allenylidene complex and, therefore, hampered the nucleophilic attack of methanol to form methoxy(alkenyl)carbenes.

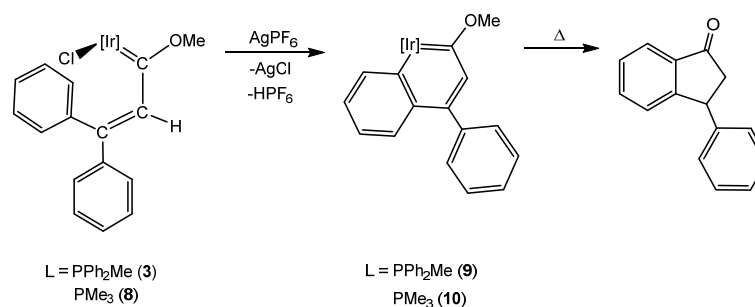
The reactivity of complex 3 towards strong bases and amines was studied. Thus, an excess of KO^tBu deprotonated the alkenyl moiety leading to the neutral methoxyallenyl complex [IrCp*Cl{C(OMe)=C=CPh₂}(PPh₂Me)] (5) (Scheme 2). This reaction is reversible, and the addition of HBF₄ regenerated cation complex 3 [9]. On the other hand, reactivity with amines did not provide the expected results. It is known that primary or secondary amines can react with alkoxy-carbenes to provide aminocarbenes through an aminolysis reaction [11–13]. However, this reaction only took place when an aqueous ammonia solution was used and the aminocarbene complex [IrCp*Cl{=C(NH₂)CH=CPh₂}(PPh₂Me)]PF₆ (6) could be isolated (Scheme 2). Instead, reactivity with amines underwent a heterolytic cleavage of the carbon(sp³)-oxygen bond to generate the acyl complex [IrCp*Cl{C(O)CH=CPh₂}(PPh₂Me)] (7) and the release of a mixture of methylammonium salts (Scheme 2) [9]. DFT calculations were performed in order to explain the different reactivity, and the presence of an equilibrium between electronic, steric and cooperative effects was revealed [14]. Calculations showed that the aminolysis reaction is not the dominant reaction with these particular alkoxy-carbene complexes.



Scheme 2. Reactivity of the methoxy(alkenyl)carbeneiridium complex **3**.

3. Iridanaphthalene Complex and Its Evolution

Besides the unexpected chemistry displayed by complex **3** towards amines, the complexes $[\text{IrCp}^*\text{Cl}=\text{C}(\text{OMe})\text{CH}=\text{CPh}_2](\text{L})\text{PF}_6$ ($\text{L} = \text{PPh}_2\text{Me}$ (**3**), PMe_3 (**8**)) [15] have been proved to be active towards orthomethylation of a phenyl substituent of the methoxy(alkenyl)carbene ligand. Thus, abstraction of the chlorido ligand, in complexes **3** and **8**, by addition of a silver salt, promoted the intramolecular C–H bond activation of a phenyl substituent of the carbene ligand, leading to the formation of a new Ir–C bond resulting in two new iridanaphthalene complexes, **9** and **10**, respectively, bearing a phenyl substituent in the iridanaphthalene moiety (Scheme 3) [16].

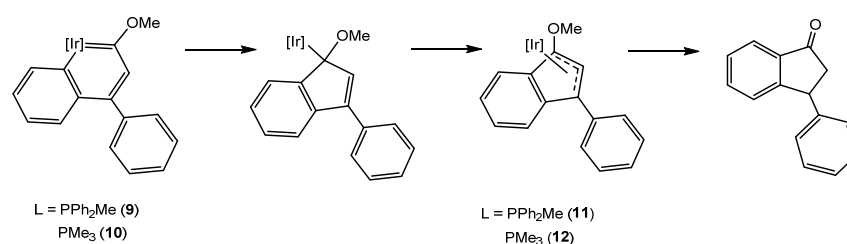


Scheme 3. Synthesis and evolution of the iridanaphthalene complexes **9** and **10**. $[\text{Ir}] = [\text{IrCp}^*\text{L}]\text{PF}_6$.

Complexes **9** and **10** represented the third example of metallanaphthalene complexes described, and the second with iridium as the transition metal [17,18]. Previously, Paneque et al. had reported the synthesis of the first iridanaphthalene complex through an oxidative ring contraction reaction of a benzannelated iridacycloheptatriene complex [18]. The X-ray structure of complexes **9**· BPh_4 , **10** and **10**· BPh_4 present C–C distances between 1.35 and 1.47 Å, comparing well with those of naphthalene, suggesting that the delocalized π -bonding extends over both rings. In these structures, the iridium atom is displaced from the nearly co-planar carbon atoms by 0.066(5) and 0.176(9) Å for **9**· BPh_4 and **10**· BPh_4 , respectively [16]. The values of the iridanaphthalene complexes with BPh_4 as counteranion are significantly smaller than those reported in the literature on other iridanaphthalene complexes, which are very similar to the value observed for **10** (0.689(5) Å) [18,19].

In the study of metallaaromatic complexes, X-ray diffraction and NMR spectroscopy are the most widely used techniques, as they provide information about the structure and nature of these complexes [20]. In complexes **9** and **10**, two features are determined in order to confirm the formation of the cycle: (i) the absence of the proton resonance of the activated C–H bond in the ^1H NMR spectra, and; (ii) the deshielding together with the C,P coupling in the carbon resonance (δ 155 ppm, $^2J_{\text{C-P}} = 10$ Hz) at the $^{13}\text{C}\{^1\text{H}\}$ NMR spectra when bonded to the iridium atom [16].

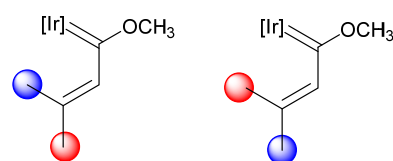
As has happened in many metallaaromatic systems, **9** and **10** resulted in the presentation of a low thermal stability. While the literature described the rearrangement of the iridaaromatic complexes into the thermodynamically stable cyclopentadienyl derivatives [21,22], complexes **9** and **10** evolved into 3-phenylindanone when heat was applied (Scheme 3) [16]. Different experiments conducted in order to elucidate the mechanism of this transformation have allowed for the observation of the expected indenyl complexes $[\text{IrCp}^*\{\eta^3\text{-(C}_9\text{H}_5\text{)(OMe)(Ph)}\}(\text{L})]\text{PF}_6$ ($\text{L} = \text{PPh}_2\text{Me}$ (**11**), PMe_3 (**12**)) as reaction intermediates. Therefore, the iridanaphthalene complexes **9** and **10** may undergo carbene migratory insertion, yielding η^1 indenyl complexes which would evolve to the η^3 intermediates **11** and **12** through a hapticity switch. Finally, the heterolytic cleavage of the O–CH₃ bond would occur and hydrogenation of the indenone would take place in order to yield the final 3-phenylindanone (Scheme 4). In order to find the hydrogen source, a reaction was also performed in deuterated solvents as well as in strictly water-free conditions. These studies suggested the involvement of the methyl group in the hydrogenation reaction [16].



Scheme 4. Mechanism proposal for the formation of 3-phenylindanone from complexes **9** and **10**. $[\text{Ir}] = [\text{IrCp}^*\text{L}]\text{PF}_6$.

4. Effect of the γ -Carbon Substituents

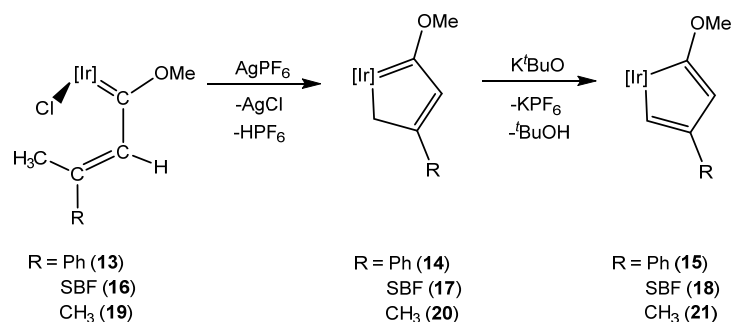
The understanding and control of the synthetic methodology, with methoxy(alkenyl) carbeneiridium complex as the starting material, will allow for the accessing of different and stable PMAHs. Thus, it was expected that the final product would depend on the substituents at a γ spatial arrangement of the precursor methoxy(alkenyl)carbeneiridium and, therefore, the key would be in the choice of the propargylic alcohol. In order to gain a better insight into the effect of the γ carbon substituent, methoxy(alkenyl)carbene complexes with two different substituents have been described, which may result in a mixture of the *E* and *Z* isomers (Scheme 5).



Scheme 5. Possible *E* and *Z* isomers in methoxy(alkenyl)carbeneiridium complexes. $[\text{Ir}] = [\text{IrCp}^*\text{Cl}(\text{PMe}_3)]^+$.

When the substituents on the γ carbon are a methyl and phenyl group (**13**), only the *E* isomer was formed, as the methyl group is located close to the iridium atom. With this spatial arrangement, AgPF_6 treatment leads to C–H bond activation of the methyl

group, obtaining the iridacyclopenta-1,3-diene complex **14** (Scheme 6). Complex **14** can react with a base in order to yield an iridacyclopenta-2,4-diene complex **15** [23]. The same behavior was observed at complex **16**, where the phenyl group was substituted with a spirobifluorene moiety (SBF) and complexes **17** and **18** were obtained (Scheme 6) [24]. Likewise, complex **19**, bearing two methyl groups, also performed the C–H bond activation, yielding **20**. After, the treatment of **20** with K^tBuO , the iridacyclopentadiene complex **21** was formed (Scheme 6). However, two hydrogen atoms on γ carbon did not afford a stable iridacyclobutadiene complex [23].



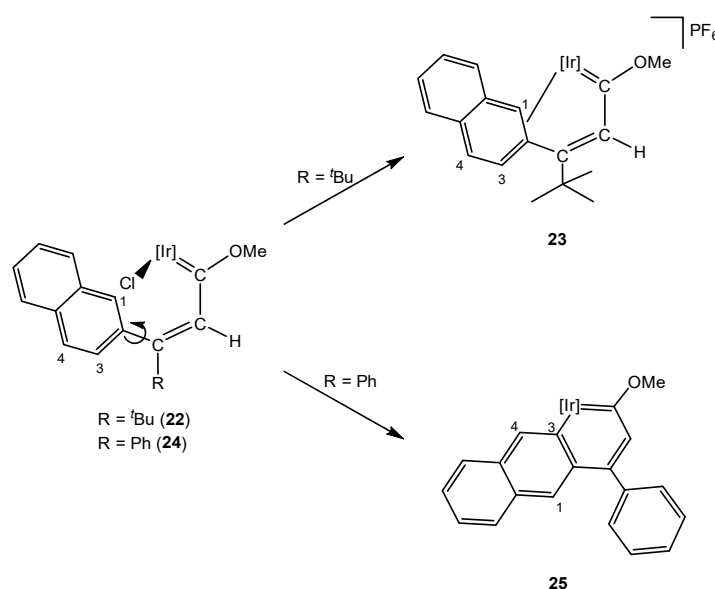
Scheme 6. Formation of iridacyclopentadiene complexes. $[\text{Ir}] = [\text{IrCp}^*(\text{PMe}_3)]\text{PF}_6$.

To better understand the importance of the isomerism at the methoxy(alkenyl)carbene for the synthesis of iridaaromatic complexes, DFT calculations were performed (B3LYP level). Thus, in complexes **13** and **16**, the calculations predicted a single product: the *E* isomer. This was due to a higher stability of the *E* isomers over the *Z* isomers in these complexes with a difference of 3.94 kcal/mol and 4.85 kcal/mol, respectively. However, if the methyl group in **16** was substituted with a phenyl group, the ΔG would be 0.70 kcal/mol which would allow for the formation of small amounts of the *Z* isomer and therefore a mixture of iridaaromatic complexes [24]. These results showed that the spatial arrangement is crucial for the methodology and that the preference of one isomer over another is clearly influenced by the lower steric hindrance.

It was not possible, in the above examples, to establish the effect that an aliphatic substituent of the γ carbon may have on the formation of the corresponding metallaaromatic compound if, instead of obtaining the *E* isomer, one had the *Z* isomer. Thus, the methoxy(alkenyl)carbene **22** bearing a 2-naphthyl and a *tert*-butyl ligand was synthesized. Due to the steric hindrance of the *tert*-butyl group, only the *E* isomer was observed, which would facilitate the C–H bond activation of the aromatic substituent. However, treatment with silver salt did not provide the expected iridaaromatic complex, and instead the η^2 complex **23** was identified (Scheme 7) [25]. Although complex **23** might be the intermediate for the formation of the iridaaromatic complex, further evolution to the corresponding iridaphenanthrene was not observed. Notably, when the *tert*-butyl substituent in **22** was replaced by a phenyl group, the C–H bond activation took place at the methoxy(alkenyl)carbene **24** and the corresponding iridaaromatic compound **25** was obtained (Scheme 7).

Fukui indices determined that C1 was the most reactive position in **22**, leading to the unique formation of **23**, despite the free rotation of the naphthalenyl substituent. In contrast, complex **24** presented the higher nucleophilic Fukui index for C4, which was too far away from the iridium nucleus (Ir–C4 distance = 5.08 Å) leading to the activation of C3 which resulted in an iridaanthracene compound, **25** (see also Section 5.3). In addition, DFT calculations (B3LYP level) determined that the C1–H bond activation of **22** to give an iridaphenanthrene complex would not be favored by 2.80 kcal/mol, possibly due to the steric hindrance of the final product. However, the effect of the *tert*-butyl moiety was further determined by comparison with complex **24** [25]. In order to analyze electronic delocalization, different methodologies exist [26–28], including the anisotropy of the induced

current density (ACID). ACID calculations showed that the electron density in **24** was delocalized along the whole system, contrary to what was observed in **22**. Similarly, the LUMO orbital for **22** was less widespread throughout the molecule than in **24** (Figure 1) and the HOMO-LUMO gap was bigger, supporting a low reactivity of the *tert*-butyl derivative. These findings endorsed the high influence of the electron density delocalization on the formation of this family of iridaaromatic complexes, which would be, therefore, promoted by second substituents such as aromatic rings.



Scheme 7. Activation of the methoxy(alkenyl)carbene complexes **22** and **24** yielding the η^2 complex **23** and the iridaaromatic complex **25**, respectively. [Ir] = [IrCp*(PMe₃)]PF₆.

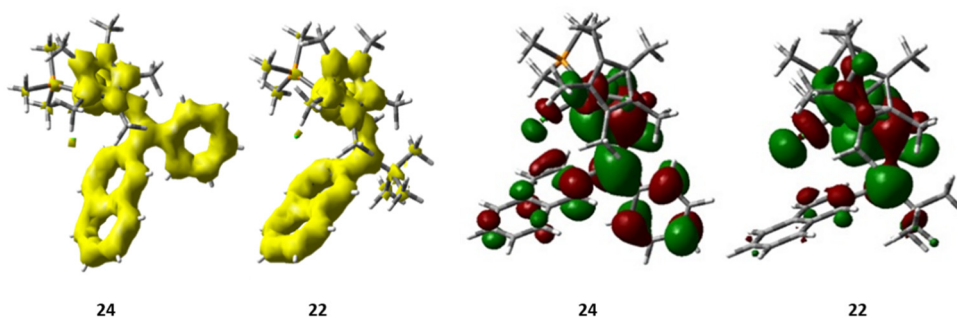


Figure 1. ACID representations (left) and LUMO orbitals (right) of complexes **22** and **24**.

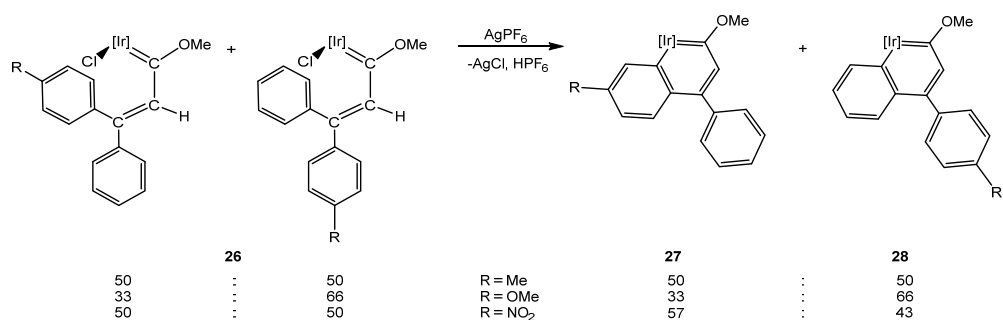
5. Stability of the Metallaaromatic Systems

Besides establishing the requirement of two aromatic substituents at the γ carbon of the methoxy(alkenyl)carbene ligand, it is also important to analyze the effect of the metal, in order to study different topologies and improve the stability of these metallaaromatics by incorporating different substituents in the aromatic cycle.

5.1. Effect of the Aromatic Ring Substituents

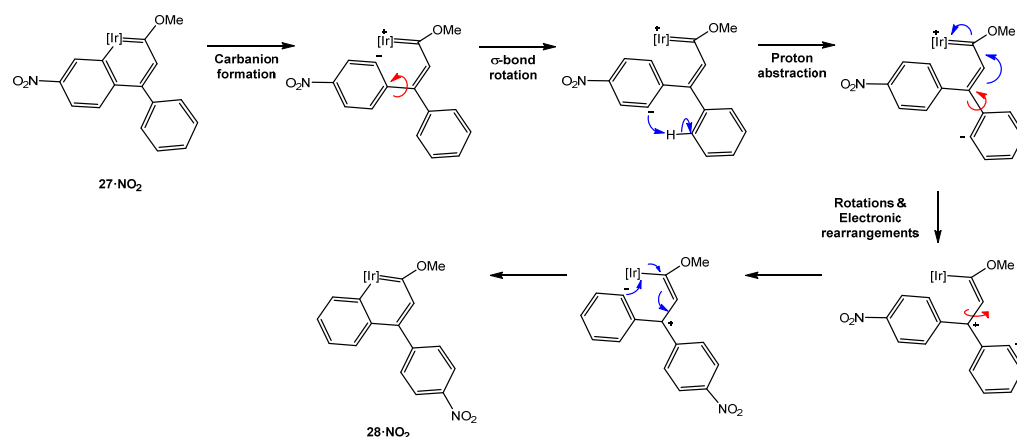
The low thermal stability of the iridanaphthalene complexes **9** and **10** (see Section 3) reduces their possible applications in materials sciences. Therefore, it is important to assess the effect of different substituents in the phenyl rings of the iridaaromatic moiety in order to enhance their stability. While Haley and co-workers reported the higher tendency to the rearrangement of iridabenzene complexes when they bear bulky ligands [21,22], our group focused on the electronic effects on the stability of the iridanaphthalene system [29].

Thus, the propargylic alcohols $\text{HC}\equiv\text{C}(\text{OH})(\text{Ph})(p\text{-R-C}_6\text{H}_4)$ with $\text{R} = \text{NO}_2$, OMe or CH_3 where chosen in order to assess the electronic effect of such substituents on the formation of the substituted 3-phenylindanone derivatives. The similar steric hindrance between the non-substituted and the nitro- or methyl-substituted phenyl rings did not allow for obtaining selectively a unique methoxy(alkenyl)carbeneiridium isomer. Consequently, the C–H bond activation reaction of the mixture of the *E*- and *Z*-isomers **26**· NO_2/CH_3 gave rise to their respective iridanaphthalenes **27** and **28** (Scheme 8). However, when one of the aromatic rings bears a methoxy group, the ratio between the *E*- and *Z*- isomers is not proportional, resulted in obtaining the *E*-isomer *E*-**26**· OMe in higher amounts, which may be due to electronic effects rather than the steric hindrance due to their location in a remote position (Scheme 8).



Scheme 8. Formation of complexes **27** and **28** from *Z/E* isomers of **26**. $[\text{Ir}] = [\text{IrCp}^*(\text{PMe}_3)]\text{PF}_6$.

As happened for **10** these mixtures of iridanaphthalene complexes are not stable in a solution evolving to the indanone derivatives [29]. The study of their evolution established a direct correlation between the electronic properties of the groups in the iridanaphthalene moiety and the final indanone, where **27**· OMe possessing a π -donor group ($-\text{OMe}$) at position 6 of the metallanaphthalene backbone proved to be the most stable iridanaphthalene. On the other hand, the nitro group is an electron-withdrawing group through resonance and induction which facilitates the isomerization of complex **27**· NO_2 into **28**· NO_2 when located in position 6 of the naphthalene ring. This process was proposed to take place through the initial formation of a carbanion from the complex **27**· NO_2 , followed by a proton abstraction right after a rotation over the σ bond between C_γ and the substituted phenyl ring. Then, the rotations and electronic rearrangements would yield complex **28**· NO_2 (Scheme 9) [29].

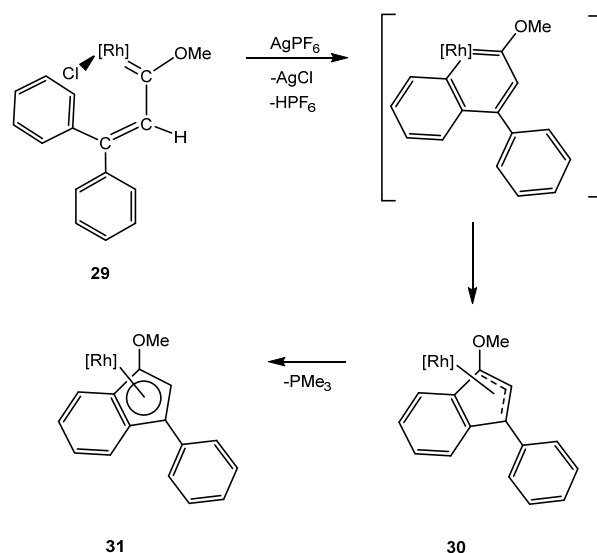


Scheme 9. Isomerization mechanism of **27**· NO_2 into **28**· NO_2 . $[\text{Ir}] = [\text{IrCp}^*(\text{PMe}_3)]\text{PF}_6$.

5.2. Effect of the Transition Metal

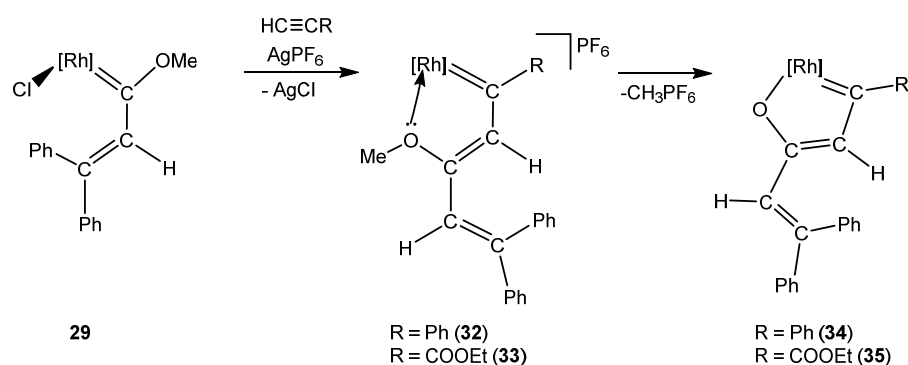
In spite of the broad range of metals used to synthesized metallabenzenes [30], their higher analogues have been mainly described with iridium [18,19,31–33] together with an example of osmium [17] and ruthenium [34]. However, rhodium, the iridium congener, has been never found to form a metallabenzene complex. This fact suggests that not only the electronic properties of the metal play a role in the synthesis of metallaaromatic complexes but also the steric ones.

In order to study the effect of the transition metal in the methodology developed for the synthesis of iridanaphthalene complexes, the methoxy(alkenyl)carbene rhodium complex **29**, analogous to **3**, was synthesized from the corresponding monoacetonitrile complex. However, treatment of complex **29** with AgPF_6 did not afford the expected rhodanaphthalene, producing instead the η^3 complex **30** together with a 15% of the η^5 complex **31**, due to the hapticity change of the indenyl ligand [35]. The formation of **30** resembles the evolution observed in the iridanaphthalene complexes **9** and **10**, which would suggest the formation of a very unstable rhodanaphthalene complex as intermediate (Scheme 10).



Scheme 10. Implementation of the methodology using rhodium as transition metal. $[\text{Rh}] = [\text{RhCp}^*(\text{PMe}_3)]\text{PF}_6$.

Although the rhodanaphthalene complexes were not possible to stabilize, the synthesis of other family of metallaaromatic complexes, the rhodafurans, was achieved. Therefore, if the reaction of **29** with the silver salt is performed in the presence of a terminal alkyne, the insertion into the $\text{Rh}=\text{C}$ bond takes place, forming the rhoda-1,3,5-hexatriene complexes **32–33** [35]. The *Z*-selectivity of complexes **32–33** would allow the intramolecular coordination of the oxygen to the rhodium nucleus, with the concomitant loss of CH_3PF_6 in order to obtain new rhodafuran complexes **34–35** (Scheme 11). These complexes represent one of the few examples of rhodafuran derivatives after Yamamoto and co-workers reported the reaction of $\text{RhCp}^*\text{Cl}_2(\text{PPh}_3)$ towards alkynes in the presence of KPF_6 and water and Tani et al. described the reactivity of alkynes with rhodium carbonyl complexes [36,37].



Scheme 11. Effect of the involvement of alkynes in the studied methodology. $[\text{Rh}] = [\text{RhCp}^*(\text{PMe}_3)]\text{PF}_6$.

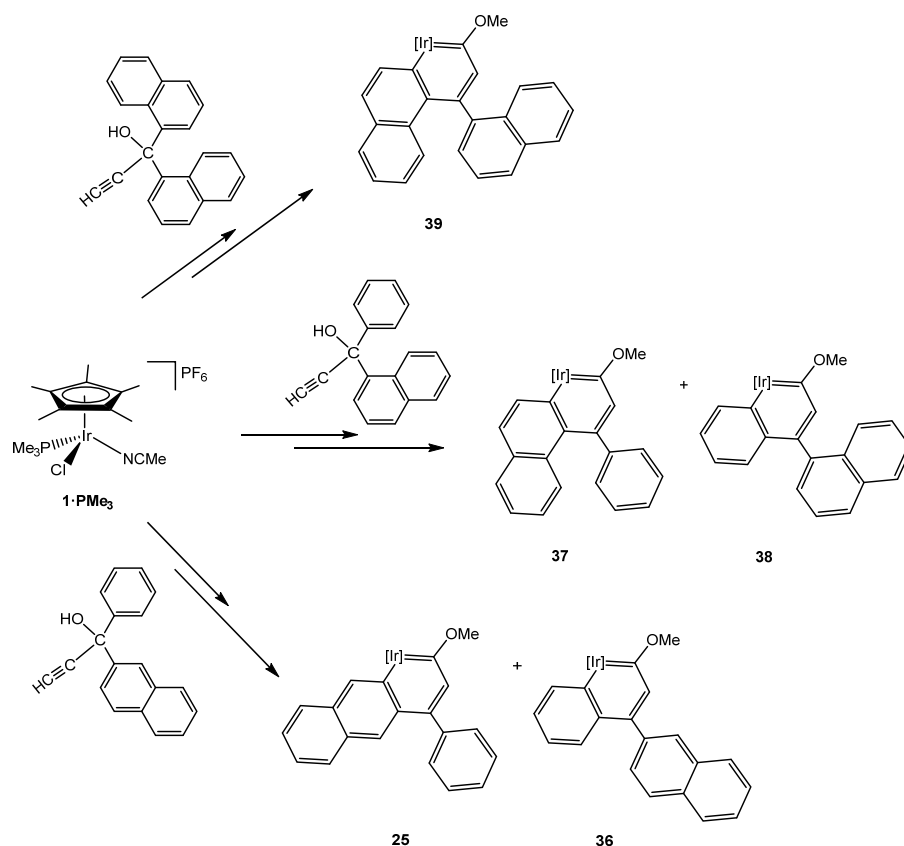
These results support the need for the use of iridium as transition metal for the synthesis of these metallanaphthalene complexes. However, the adjustment of the methodology by including terminal alkynes allows for a new and versatile way of achieving the synthesis of rhodafurans with a broad range of substituents.

5.3. Effect of the Topology

In spite of the successful development of the methodology in the synthesis of iridanaphthalenes, the synthesis of larger structures is necessary in order to improve the properties of PAHs. However, the development of higher analogues of metallanaphthalene is a barely-studied field and only a few examples are known [32–34,38].

In order to obtain higher analogues, such as iridaanthracene or iridaphenantrene derivatives, propargylic alcohols bearing at least one naphthyl group at γ position were synthesized. As was stated in Section 4, the *E/Z* isomerism at the methoxy(alkenyl)carbeneiridium complexes is crucial, however, the steric hindrance difference between a phenyl and a naphthyl substituents is not high enough to hamper the formation of both isomers and, consequently, the corresponding iridaaromatics (Scheme 12) [39].

However, the naphthyl group can be bonded to the γ carbon through two different positions, leading to a variety of products. On the one hand, when coordinated at 2-position, an iridaanthracene complex **25** and the iridanaphthalene complex **36** were obtained (Scheme 12, bottom) [25]. Complex **25** represents the second example of a metallaanthracene described in literature. Frogley and Wright reported in 2016 the first metallaanthracene complex, also bearing iridium as metal center [32]. In contrast to the α -iridaanthracene complex **25**, Wright's complex is a tethered- β -iridaanthracene. Although it was not possible to obtain X-ray data of **25**, its geometry optimization by DFT calculations showed that both iridaanthracene complexes show similar structural data which are also comparable to the purely organic anthracene. Regarding **25**, DFT calculations determined that two rotational isomers for the corresponding methoxy(alkenyl)carbene complex **24** were possible, due to the free rotation of the naphthyl substituent (Figure 2). This effect would lead to not only **25**, but also an iridaphenantrene derivative **25b**, which was never experimentally observed. Although DFT calculations showed that the most stable rotational isomer was the precursor of the iridaphenantrene complex, the energy difference of the isomers was too small ($\Delta G = 0.88$ kcal/mol) compared to the higher stability of **25**, which is 6.41 kcal/mol more stable than **25b**, probably due to the larger steric hindrance of **25b** (Figure 2) [25].



Scheme 12. Synthesis of higher analogues $[Ir] = [IrCp^*(PMe_3)]PF_6$.

On the other hand, the naphthyl group can be bonded at 1-position getting rid of the rotational isomerism.

Thus, despite the steric hindrance, activation at the C–H bond of the 1-naphthyl substituent led to the first iridaphenanthrene complex **37** (Scheme 12, middle) [39]. Interestingly, the activation at the phenyl group gave rise to two diastereoisomers for the iridabinnaphthyl complex **38**, observable by NMR spectroscopy, due to the hindered rotation about the biaryl bond as well as the iridium chiral center. This atropisomerism was also found in the iridaphenanthrene complex **39** formed by the activation of a symmetric propargylic alcohol bearing two 1-naphthyl substituents (Scheme 12, top) [39]. A theoretical study determined that the rotational barriers around the biaryl bond in **38** and **39**, as well as their aromaticity, are comparable to the 1,1'-binaphthalene and the calculated energy differences between *S,M* and *S,P* isomers can be related to the experimentally observed product ratios [39]. Prior to the formation of **37** and **39**, low temperature studies allowed for the characterization of the corresponding η^2 intermediates, which in contrast to complex **23** (see Section 4), were capable of performing the C–H bond activation in order to obtain the iridaaromatic complexes.

In addition, Liu et al. applied our methodology in order to obtain iridafluoranthene derivatives (Scheme 13) [33]. Thus, methoxy(alkenyl)carbene complexes, such as **40** and **42**, are capable of performing C–H bond activation in order to give the iridaaromatic complexes **41** and **43**, respectively. Interestingly, when an asymmetric propargylic alcohol is used, only one methoxy(alkenyl)carbene iridium complex **42** is obtained, and therefore, only one iridafluoranthene complex **43**. The authors proposed the unlikely activation of the remote fused ring to provide a seven-member metallacycle, which might be less favored than the obtained six-member ring [33]. This selectivity is consistent with our theoretical and experimental work using aromatic moieties at γ carbon with the *ortho* positions substituted (see Section 5.4) [40], as well as the effect of their steric hindrance, which would hinder the formation of the other *Z*-isomer.

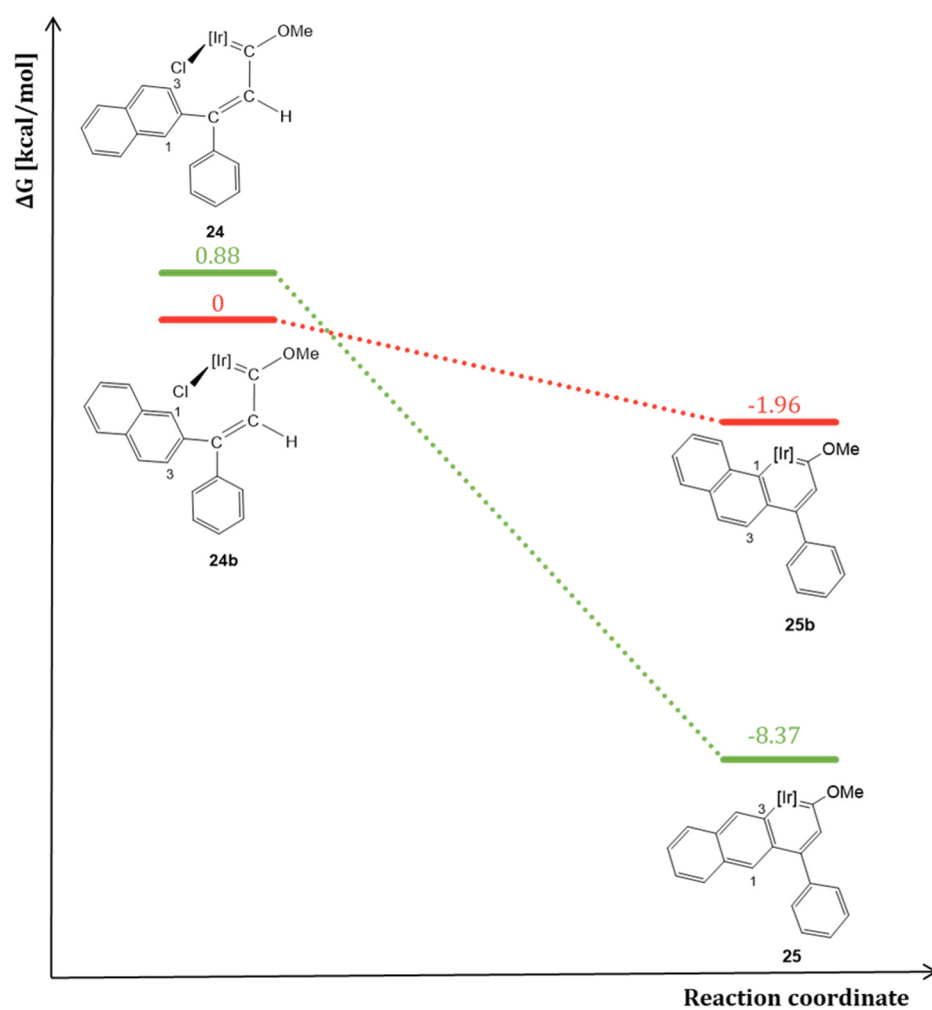
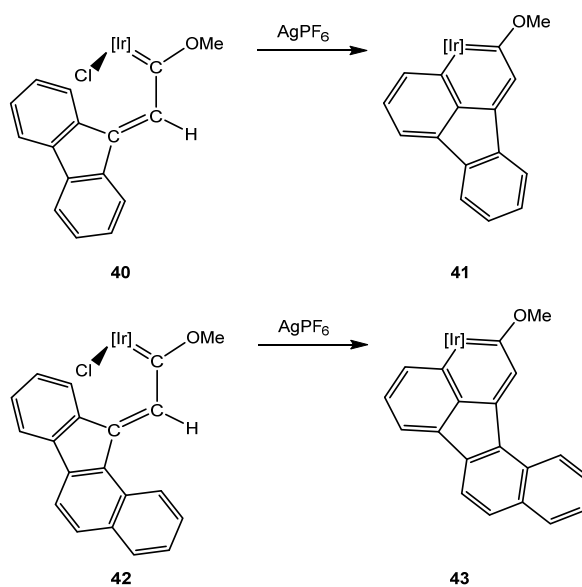


Figure 2. Energy profile for the formation of iridaanthracene complex **25** vs. iridaphenanthrene complex **25b** [Ir] = [IrCp*(PMe₃)]PF₆.



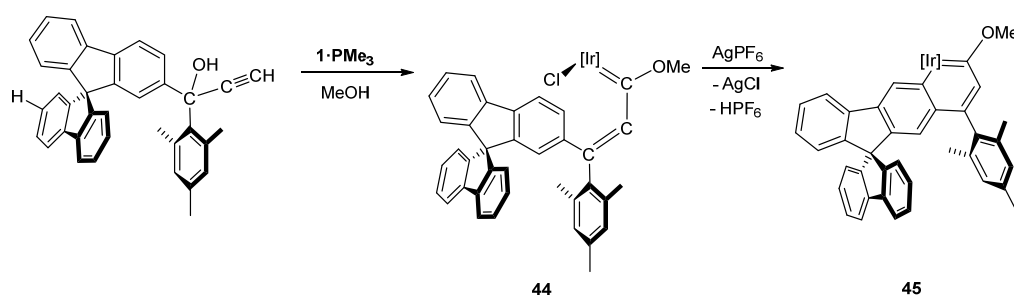
Scheme 13. Synthesis of some iridafluoranthene derivatives. [Ir] = [IrCp*(PMe₃)]PF₆.

The iridafluoranthene complexes showed a red-shift in the UV-Vis spectra for the higher conjugated derivatives such as **43**, while substitution at **41** did not have effect. In addition, CV measurements showed that only the first reduction was reversible. The substitution with electron-donating or electron-withdrawing groups at **41** caused a cathodic or anodic shift in the reduction potential, respectively, while **43** derivatives showed anode shift for the reduction and cathode shift for the oxidation potentials [33].

5.4. Special Systems

The chemistry of metallaaromatic complexes is not only limited to metallabenzenes, metallanaphthalenes or higher analogues [30,41–45]. As has been previously described by other groups, different topologies can produce properties which could be used in specific applications [30,43,46]. Therefore, the introduction of systems such as the spirobifluorene moiety (SBF) could be useful to generate new properties with optoelectronic applications.

As described in Section 4, the higher steric hindrance of the SBF substituent with respect to the methyl group, was the key for the formation of the methoxy(alkenyl)carbene isomer **16** and, therefore, a five-membered metallacycle **17** upon C–H bond activation [24]. If the methyl group is substituted by a mesityl group, the *E* methoxy(alkenyl)carbene isomer with the SBF moiety near the iridium atom, **44**, is 1.85 kcal/mol more stable than the *Z* isomer [24], which leads to a selective synthesis of **44**. Subsequent activation of the C–H bond led to the first spirobifluorene metallaaromatic complex **45** (Scheme 14) [40].



Scheme 14. Spirobifluorene containing complexes. [Ir] = [IrCp*(PMe₃)]PF₆.

Complex **45** showed interesting properties as a potential material in optoelectronics. It presented a high thermal stability above 473 K and higher aromatic character, as well as a hindered rotational barrier 20 times higher than biaryl systems **38** and **39**. In addition, a 1.1 eV red-shift in the UV/Vis spectrum compared to the spirobifluorene was also observed [40].

6. Conclusions

In recent years our versatile synthetic methodology has allowed us to obtain different topologies of metallaaromatic complexes, such as iridanaphthalenes, iridaphenanthrenes, iridanthracene, rhodafurans or the spirobifluorene iridanaphthalene.

The key aspect of our methodology is the precursor, a methoxy(alkenyl)carbene complex, which by C–H bond activation of one of the *ortho* carbons of an aromatic substituent on γ carbon leads to the formation of a metallaaromatic compound. In order to guarantee the success of this methodology, we have studied the influence of different substituents at the γ carbon, the metallic center, the substituents on the aromatic cycle and the possibility of using it to obtain different topologies. Therefore, it was concluded that: (1) it is necessary for one of the substituents on the γ carbon to possess a large steric hindrance in order to obtain a single *Z* or *E* isomer; (2) the existence of a second substituent, also aromatic, ensures the formation of the metallaaromatic complex due to its capability to delocalize the electronic density among the whole complex; (3) in this case, at least one of them need not be substituted in the *ortho* positions; (4) the increase of aromatic rings increases stability; (5) the most favored *ortho* position for C–H bond activation is the one that produces the least

stressed cycle; and (6) the capacity of the methodology to synthesize different topologies is very broad.

All together gives the opportunity to synthesize analogues to polycyclic aromatic hydrocarbons, PMAHs, which are small fragments of graphene doped with a transition metal and thus to study their new properties and consequently their applications in the field of materials.

Author Contributions: Writing—original draft preparation, M.T., S.B.; writing—review and editing, M.T., S.B.; visualization, M.T., S.B.; funding acquisition, S.B. All authors have read and agreed to the published version of the manuscript.

Funding: This research was funded by Xunta de Galicia (ED431F 2016/005) and IBEROS (0245_IBERO S_1_E).

Acknowledgments: The authors acknowledge collaborations and fruitful discussions in this research area with Jorge Bravo and Soledad García-Fontán (UVigo) and the FA3 group of the Universidade de Vigo and thank them for all their support. Important contributions to these experimental and theoretical studies have been made by many coworkers and students, mainly Ángeles Peña-Gallego, José L. Alonso Gómez, Raquel Pereira-Cameselle, Jesús Castro, José M. Hermida-Ramón, Vanesa Arias-Coronado as well as Krystal M. Cid-Seara. The authors are thankful to the Supercomputing Center of Galicia (CESGA) for the generous allocation of computer time and Universidade de Vigo-CACTI services for recording the NMR and UV/Vis spectra and collecting X-ray data.

Conflicts of Interest: The authors declare no conflict of interest.

References and Note

1. Eftekhari, A.; Garcia, H. The necessity of structural irregularities for the chemical applications of graphene. *Mater. Today Chem.* **2017**, *4*, 1–16. [[CrossRef](#)]
2. Rieger, R.; Müllen, K. Forever young: Polycyclic aromatic hydrocarbons as model cases for structural and optical studies. *J. Phys. Org. Chem.* **2010**, *23*, 315–325. [[CrossRef](#)]
3. Stępień, M.; Gońka, E.; Żyła, M.; Sprutta, N. Heterocyclic Nanographenes and Other Polycyclic Heteroaromatic Compounds: Synthetic Routes, Properties, and Applications. *Chem. Rev.* **2017**, *117*, 3479–3716. [[CrossRef](#)] [[PubMed](#)]
4. Castro-Fernández, S.; Cruz, C.M.; Mariz, I.F.A.; Márquez, I.R.; Jiménez, V.G.; Palomino-Ruiz, L.; Cuerva, J.M.; Maçôas, E.; Campaña, A.G. Two-Photon Absorption Enhancement by the Inclusion of a Tropone Ring in Distorted Nanographene Ribbons. *Angew. Chem. Int. Ed.* **2020**, *59*, 7139–7145. [[CrossRef](#)] [[PubMed](#)]
5. Medel, M.A.; Tapia, R.; Blanco, V.; Miguel, D.; Morcillo, S.P.; Campaña, A.G. Octagon-Embedded Carbohelicene as a Chiral Motif for Circularly Polarized Luminescence Emission of Saddle-Helix Nanographenes. *Angew. Chem. Int. Ed.* **2021**, *60*, 6094–6100. [[CrossRef](#)] [[PubMed](#)]
6. Roh, S.W.; Choi, K.; Lee, C. Transition Metal Vinylidene- and Allenylidene-Mediated Catalysis in Organic Synthesis. *Chem. Rev.* **2019**, *119*, 4293–4356. [[CrossRef](#)] [[PubMed](#)]
7. Cadierno, V.; Gamasa, M.P.; Gimeno, J. Recent Developments in the Reactivity of Allenylidene and Cumulenylidene Complexes. *Eur. J. Inorg. Chem.* **2001**, 571–591. [[CrossRef](#)]
8. Puerta, M.C.; Valerga, P. Ruthenium and osmium vinylidene complexes and some related compounds. *Coord. Chem. Rev.* **1999**, *193–195*, 977–1025. [[CrossRef](#)]
9. Talavera, M.; Bolaño, S.; Bravo, J.; Castro, J.; García-Fontán, S.; Hermida-Ramón, J.M. Nucleophilic Attack in Methoxycarbenes: Heterolytic Cleavage of the Carbon (sp^3)–Oxygen Bond versus Aminolysis. *Organometallics* **2013**, *32*, 4402–4408. [[CrossRef](#)]
10. Talavera, M.; Bravo, J.; Gonsalvi, L.; Peruzzini, M.; Zuccaccia, C.; Bolaño, S. $[\text{IrCp}^*(\text{NCMe})_2(\text{PPh}_2\text{Me})][\text{PF}_6]_2$ as Catalyst for the Meyer–Schuster Rearrangement of Arylpropargylic Alcohols under Mild Conditions. *Eur. J. Inorg. Chem.* **2014**, 6268–6274. [[CrossRef](#)]
11. Feliciano, A.; Padilla, R.; Escalante, C.H.; Herbert-Pucheta, J.E.; Vázquez, M.A.; Tamariz, J.; Delgado, F. Synthesis of novel 2,5-substituted p-aminophenols and 2,5-substituted p-quinones in a one-pot reaction between α -alkoxyvinyl(ethoxy)carbene complexes, amines and alkynes. *J. Organomet. Chem.* **2020**, *923*, 121360. [[CrossRef](#)]
12. Andrada, D.M.; Jimenez-Halla, J.O.C.; Solà, M. Mechanism of the Aminolysis of Fischer Alkoxy and Thiocarbene Complexes: A DFT Study. *J. Org. Chem.* **2010**, *75*, 5821–5836. [[CrossRef](#)] [[PubMed](#)]
13. Ulrich, K.; Porhiel, E.; Péron, V.; Ferrand, V.; Le Bozec, H. Functionalised alkenylcarbene metal complexes ($M=\text{Ru}$, W , Cr) by activation of propargyl alcohol derivatives. *J. Organomet. Chem.* **2000**, *601*, 78–86. [[CrossRef](#)]
14. Talavera, M.; Bolaño, S.; Bravo, J.; García-Fontán, S.; Hermida-Ramón, J.M. The Catalytic Role of Extra Molecules in the Aminolysis or Heterolytic Cleavage of an Iridium Alkoxy-carbene Complex. *Eur. J. Inorg. Chem.* **2015**, 4024–4031. [[CrossRef](#)]
15. Note that the synthesis of complex **8** was performed following the same methodology than for complex **3**.
16. Talavera, M.; Bolaño, S.; Bravo, J.; Castro, J.; García-Fontán, S.; Hermida-Ramón, J.M. Formation of Indanone from an Iridanaphthalene Complex. *Organometallics* **2013**, *32*, 4058–4060. [[CrossRef](#)]

17. Liu, B.; Xie, H.; Wang, H.; Wu, L.; Zhao, Q.; Chen, J.; Wen, T.B.; Cao, Z.; Xia, H. Selective Synthesis of Osmanaphthalene and Osmanaphthalene by Intramolecular C–H Activation. *Angew. Chem. Int. Ed.* **2009**, *48*, 5461–5464. [[CrossRef](#)]
18. Paneque, M.; Posadas, C.M.; Poveda, M.L.; Rendón, N.; Santos, L.L.; Álvarez, E.; Salazar, V.; Mereiter, K.; Oñate, E. Metallacycloheptatrienes of Iridium(III): Synthesis and Reactivity. *Organometallics* **2007**, *26*, 3403–3415. [[CrossRef](#)]
19. Vivancos, Á.; Hernández, Y.A.; Paneque, M.; Poveda, M.L.; Salazar, V.; Álvarez, E. Formation of β -Metallanaphthalenes by the Coupling of a Benzo-Iridacyclopentadiene with Olefins. *Organometallics* **2015**, *34*, 177–188. [[CrossRef](#)]
20. Mitchell, R.H. Measuring Aromaticity by NMR. *Chem. Rev.* **2001**, *101*, 1301–1316. [[CrossRef](#)]
21. Wu, H.-P.; Weakley, T.J.R.; Haley, M.M. Regioselective Formation of β -Alkyl- α -phenyliridabenzene via Unsymmetrical 3-Vinylcyclopropenes: Probing Steric and Electronic Influences by Varying the Alkyl Ring Substituent. *Chem. Eur. J.* **2005**, *11*, 1191–1200. [[CrossRef](#)]
22. Wu, H.-P.; Ess, D.H.; Lanza, S.; Weakley, T.J.R.; Houk, K.N.; Baldrige, K.K.; Haley, M.M. Rearrangement of Iridabenzvalenes to Iridabenzene and/or η^5 -Cyclopentadienyliridium(I) Complexes: Experimental and Computational Analysis of the Influence of Silyl Ring Substituents and Phosphine Ligands. *Organometallics* **2007**, *26*, 3957–3968. [[CrossRef](#)]
23. Talavera, M.; Bolaño, S.; Bravo, J.; Castro, J.; García-Fontán, S. Cyclometalated Iridium Complexes from Intramolecular C–H Activation of $[\text{IrCp}^*\text{Cl}\{\text{C}(\text{OMe})\text{CH}=\text{C}(\text{CH}_3)\text{R}\}\text{L}]$ (R = CH₃, Ph; L = PPh₂Me, PMe₃). *Organometallics* **2013**, *32*, 7241–7244. [[CrossRef](#)]
24. Pereira-Cameselle, R.; Peña-Gallego, Á.; Cid-Seara, K.M.; Alonso-Gómez, J.L.; Talavera, M.; Bolaño, S. Chemoselectivity on the synthesis of iridacycles: A theoretical and experimental study. *Inorg. Chim. Acta* **2020**, *517*, 120189. [[CrossRef](#)]
25. Talavera, M.; Cid-Seara, K.M.; Peña-Gallego, A.; Bolano, S. Key factors in the synthesis of polycyclic iridaaromatics via the methoxyalkenylcarbene pathway. *Dalton Trans.* **2021**. [[CrossRef](#)]
26. Szczepanik, D.W.; Solà, M. 8-The electron density of delocalized bonds (EDDBs) as a measure of local and global aromaticity. In *Aromaticity*; Fernandez, I., Ed.; Elsevier: Amsterdam, The Netherlands, 2021; pp. 259–284.
27. Geuenich, D.; Hess, K.; Köhler, F.; Herges, R. Anisotropy of the Induced Current Density (ACID), a General Method To Quantify and Visualize Electronic Delocalization. *Chem. Rev.* **2005**, *105*, 3758–3772. [[CrossRef](#)] [[PubMed](#)]
28. Szczepanik, D.W.; Solà, M. Electron Delocalization in Planar Metallacycles: Hückel or Möbius Aromatic? *ChemistryOpen* **2019**, *8*, 219–227. [[CrossRef](#)] [[PubMed](#)]
29. Talavera, M.; Bravo, J.; Castro, J.; Garcia-Fontan, S.; Hermida-Ramon, J.M.; Bolano, S. Electronic effects of substituents on the stability of the iridanaphthalene compound $[\text{IrCp}^*\{\text{C}(\text{OMe})\text{CH}=\text{C}(\text{o-C}_6\text{H}_4)(\text{Ph})\}(\text{PMe}_3)]\text{PF}_6$. *Dalton Trans.* **2014**, *43*, 17366–17374. [[CrossRef](#)] [[PubMed](#)]
30. Chen, D.; Hua, Y.; Xia, H. Metallaaromatic Chemistry: History and Development. *Chem. Rev.* **2020**, *120*, 12994–13086. [[CrossRef](#)]
31. Paneque, M.; Poveda, M.L.; Rendón, N. Synthesis and Reactivity of Iridacycles Containing the TpMe₂Ir Moiety. *Eur. J. Inorg. Chem.* **2011**, 19–33. [[CrossRef](#)]
32. Frogley, B.J.; Wright, L.J. A Metallaanthracene and Derived Metallaanthraquinone. *Angew. Chem. Int. Ed.* **2017**, *56*, 143–147. [[CrossRef](#)] [[PubMed](#)]
33. Hu, Y.X.; Zhang, J.; Wang, X.; Lu, Z.; Zhang, F.; Yang, X.; Ma, Z.; Yin, J.; Xia, H.; Liu, S.H. One-pot syntheses of irida-polycyclic aromatic hydrocarbons. *Chem. Sci.* **2019**, *10*, 10894–10899. [[CrossRef](#)] [[PubMed](#)]
34. Yang, J.; Jones, W.M.; Dixon, J.K.; Allison, N.T. Detection of a Ruthenabenzene, Ruthenaphenoxide, and Ruthenaphenanthrene Oxide: The First Metalla Aromatics of a Second-Row Transition Metal. *J. Am. Chem. Soc.* **1995**, *117*, 9776–9777. [[CrossRef](#)]
35. Talavera, M.; Pereira-Cameselle, R.; Bolaño, S. Rhodafuran from a methoxy(alkenyl)carbene by the rhoda-1,3,5-hexatriene route. *Dalton Trans.* **2018**, *47*, 9064–9071. [[CrossRef](#)] [[PubMed](#)]
36. Kataoka, Y.; Iwato, Y.; Shibahara, A.; Yamagata, T.; Tani, K. Configurationally stable metal-centered chirality: Stereospecific and regioselective rhodaacylation of alkynes controlled by the third generation of the $[\text{Cp}^*\text{-P}]\text{H}$ ligand. *Chem. Commun.* **2000**, *10*, 841–842. [[CrossRef](#)]
37. Ogata, K.; Kuge, K.; Tatsumi, K.; Yamamoto, Y. One-step synthesis of alkenyl ketone complexes from $\text{Cp}^*\text{RhCl}_2(\text{PPh}_3)$, alkyne and H₂O in the presence of KPF₆. *Chem. Commun.* **2002**, *2*, 128–129.
38. Mike, C.A.; Ferde, R.; Allison, N.T. Evidence for rhenaphenanthrene formation and its conversion to fluorenone. *Organometallics* **1988**, *7*, 1457–1459. [[CrossRef](#)]
39. Talavera, M.; Peña-Gallego, A.; Alonso-Gómez, J.L.; Bolaño, S. Metallaaromatic biaryl atropisomers. *Chem. Commun.* **2018**, *54*, 10974–10976. [[CrossRef](#)]
40. Arias-Coronado, V.C.; Pereira-Cameselle, R.; Ozcelik, A.; Talavera, M.; Peña-Gallego, Á.; Alonso-Gómez, J.L.; Bolaño, S. Spirobifluorene Metallaaromatics. *Chem. Eur. J.* **2019**, *25*, 13496–13499. [[CrossRef](#)]
41. Cao, X.-Y.; Zhao, Q.; Lin, Z.; Xia, H. The Chemistry of Aromatic Osmacycles. *Acc. Chem. Res.* **2014**, *47*, 341–354. [[CrossRef](#)]
42. Ma, W.; Yu, C.; Chen, T.; Xu, L.; Zhang, W.-X.; Xi, Z. Metallacyclopentadienes: Synthesis, structure and reactivity. *Chem. Soc. Rev.* **2017**, *46*, 1160–1192. [[CrossRef](#)]
43. Frogley, B.J.; Wright, L.J. Recent Advances in Metallaaromatic Chemistry. *Chem. Eur. J.* **2018**, *24*, 2025–2038. [[CrossRef](#)] [[PubMed](#)]
44. Frogley, B.J.; Wright, L.J. Fused-ring metallabenzene. *Coord. Chem. Rev.* **2014**, *270–271*, 151–166. [[CrossRef](#)]
45. Jia, G. Our Journey to the Chemistry of Metallabenzynes. *Organometallics* **2013**, *32*, 6852–6866. [[CrossRef](#)]
46. Zhu, C.; Xia, H. Carbolong Chemistry: A Story of Carbon Chain Ligands and Transition Metals. *Acc. Chem. Res.* **2018**, *51*, 1691–1700. [[CrossRef](#)] [[PubMed](#)]